Journal of Applied Biomedicine

Original research article

Amaryllidaceae alkaloids in skin cancer management: Photoprotective effect on human keratinocytes and anti-proliferative activity in melanoma cells

Carol Castañeda [1], Karent Bravo [1], Natalie Cortés [1,2], Janeth Bedoya [3], Warley de S. Borges [4], Jaume Bastida [5], Edison Osorio [1] *

[1] *Universidad de Antioquía, Facultad de Ciencias Farmacéuticas y Alimentarias, Grupo de Investigación en Sustancias Bioactivas, Medellín, Colombia*

[2] *Universidad de Ibagué, Facultad de Ciencias Naturales y Matemáticas, Ibagué, Colombia*

[3] *Universidad de Antioquia, Facultad de Medicina, Grupo Medicina Molecular y de Translación, Medellín, Colombia*

[4] *Universidade Federal do Espírito Santo, Departamento de Química, Vitória, Espírito Santo, Brazil*

[5] *Universitat de Barcelona, Facultat de Farmàcia i Ciències de l'Alimentació, Departament de Biologia, Sanitat i Medi Ambient, Barcelona, Spain*

Abstract

Skin cancer has high rates of mortality and therapeutic failure. In this study, to develop a multi-agent strategy for skin cancer management, the selective cytotoxicity of several alkaloid fractions and pure alkaloids isolated from Amaryllidaceae species was evaluated in melanoma cells. In addition, UVB-stimulated keratinocytes (HaCaT) were exposed to seven alkaloid fractions characterized by GC-MS, and the production of intracellular reactive oxygen species (ROS) and IL-6, were measured to evaluate their photoprotection effects. The *Eucharis caucana* (bulb) alkaloid fraction (20 μg/ml) had a clear effect on the viability of melanoma cells, reducing it by 45.7% without affecting healthy keratinocytes. This alkaloid fraction and tazettine (both at 2.5 μg/ml) suppressed UVB-induced ROS production by 31.6% and 29.4%, respectively. The highest anti-inflammatory potential was shown by the *Zephyranthes carinata* (bulb) alkaloid fraction (10 μg/ml), which reduced IL-6 production by 90.8%. According to the chemometric analysis, lycoramine and tazettine had a photoprotective effect on the UVB-exposed HaCaT cells, attenuating the production of ROS and IL-6. These results suggest that Amaryllidaceae alkaloids have photoprotective and therapeutic potential in skin cancer management, especially at low concentrations.

Keywords: Amaryllidaceae alkaloids; *Eucharis caucana*; Photoprotection; Skin cancer; *Zephyranthes carinata*

Highlights:
- A multi-agent strategy for skin cancer management is urgently required.
- *Eucharis caucana* alkaloid fraction and tazettine suppressed UVB-induced ROS production.
- *Zephyranthes carinata* alkaloid fraction showed the highest anti-inflammatory potential.
- Lycoramine and tazettine had a photoprotective effect on the UVB-exposed HaCaT cells.
- Amaryllidaceae alkaloids have photoprotective and therapeutic potential in skin cancer management.

Introduction

The skin is a physical and microbiological barrier that provides the body with protection, sensations, and thermal isolation. Its frequent cell replacement, wide surface area, and consequent exposure to environmental risk factors render it a very susceptible tissue for cancer development (Apalla et al., 2017a; Oak et al., 2018). There are two types of skin cancer: melanoma, which is the most aggressive and occurs in melanocytes, and non-melanoma skin cancers (NMSC), which develop in keratinocytes in the epidermal basal layer (basal cell carcinoma) or spinous layer (epidermoid carcinoma) (Real and López, 2016).

NMSC are the most common cause of malignant tumors in light-skinned people. Epidemiological data indicate that the incidence of melanoma is growing by around 2.6% per year. In 2020, there were 324,635 new cases of melanoma in the world and 57,043 deaths. Although NMSC have low mortality rates, their incidence is 18–20 times higher than melanoma (Apalla et al., 2017b; Sung et al., 2021) and their exclusion from large cancer registers results in limited epidemiological data. The rise in the incidence of skin cancer is strongly associated with occupational and recreational activities that involve exposure to ultraviolet B (UVB) radiation and with the decay of the ozone layer (Gordon, 2013; Oak et al., 2018).

The most dangerous risk factor for skin cancer is UVB radiation (Apalla et al., 2017a). In particular, UVB rays can break DNA strands and release toxic photoproducts capable of inducing mutations in *p53*, a tumor-suppressor gene, and activate the expression of cell growth-promoting proto-oncogenes and the MAPK signaling pathway, which plays a key role in primary and metastatic melanoma (Kozma and Eide, 2014). UVB radiation also triggers signaling pathways related to the production of reactive oxygen species (ROS), pro-inflammatory cytokines, carcinogenic factor expression, and immunological suppression, which prevents tissue regeneration and repair, and promotes tumor growth (Montes de Oca et al., 2017; Voiculescu et al., 2019).

The available drugs for skin cancer management have relatively low therapeutic response rates (20–48%), depending on the type of injury, location, and stage. Recently approved immunotherapeutic drugs are more effective, but they are associated with dermatitis, hepatitis, endocrinopathies, and even the appearance of other types of cancer (Apalla et al., 2017a; Nieweg and Gallegos-Hernández, 2016). Considering the rising incidence of skin cancers and the limitations of available therapies, there is a need to develop new alternatives for their prevention and treatment. Cancer drug discovery has found an ample number of bioactive compounds from natural sources, the origin of 46% of anticancer drugs approved in the last 40 years (Lu and Wang, 2020; Newman and Cragg, 2020). Interestingly, many of these compounds correspond to alkaloids. These include vincristine and vinblastine (from *Catharanthus roseus*), used for myeloid leukemia treatment; other alkaloids such as topotecan and camptothecin (from *Camptoteca accuminata*), both used to treat lung, colon, and breast cancer; or homoharringtonine (from *Cephalotaxus fortunei*), used to treat chronic myeloid leukemia (Newman and Cragg, 2020; Roussi et al., 2012). In addition, natural product drugs or semisynthetic analog drugs containing nitrogen in their structure – from microbes such as bleomycin, peplomycin, romidepsin, and staurosporin, or from organisms of marine origin such as aplidine, cytarabine, and trabectedin – are also widely used as potent anticancer drugs for various cancers (Cragg and Pezzuto, 2016; Newman and Cragg, 2020). In fact, alkaloids represent 50% of naturally occurring compounds that have pharmaceutical application, hence their importance in drug research (Howes, 2018; Qiu et al., 2014).

Several molecules with antitumoral potential are found among the Amaryllidaceae alkaloids (AA) (Nair et al., 2016a). The AA are a distinctive chemotaxonomic feature of plants of the subfamily Amaryllidoideae, and the family Amaryllidaceae, with 636 alkaloids identified to date (Berkov et al., 2020). These plants are widely distributed in tropical and subtropical zones, especially in Africa and South America (Bastida et al., 2006). Early historical references mention Hippocrates and Sorano of Ephesus using *Narcissus poeticus* extracts to treat uterine tumors (Kornienko and Evidente, 2008). In more recent studies, AA have been isolated and tested as anti-proliferative agents for different types of cancer (Nair et al., 2016b), but their activity in skin models is not well-established. The search for new molecules for the treatment and prevention of skin cancer has led to the evaluation of the potential of alkaloid fractions from *Crinum jagus* (J. Thomps.) Dandy, *Eucharis caucana* Meerow, *Hippeastrum elegans* (Spreng.) H. E. Moore, and *Zephyranthes carinata* Herb., as well as pure AA obtained from previously investigated plants, to modulate UVB-induced oxidative stress and inflammation in healthy human keratinocytes. The antiproliferative and antimetastatic activity of these substances was also assessed in metastatic melanoma cells.

Materials and methods

Chemical analysis

Plant material
C. jagus and *Z. carinata* specimens were collected in the department of Antioquia-Colombia. *E. caucana* in Choco-Colombia and *H. elegans* in Casanare-Colombia, during the flowering period between February and April 2014. The collected species were identified with voucher numbers. A voucher specimen was maintained in the herbarium of the University of Antioquia. The species studied were collected with authorization from the Ministry of Environment with a genetic resource access contract #328. The collected plant material was dried in an oven at 40 °C for several days and powdered before extraction.

Alkaloid extraction
Samples (approximately 300 g dry powdered material) from bulbs (B) and leaves (L) underwent exhaustive extraction with methanol. The solvent was evaporated under vacuum conditions, and the residues were dissolved in 30 ml of 2% sulfuric acid and defatted five times with 40 ml ethyl acetate. The aqueous layers were then basified with 25% ammonia to pH 9.5–10.0, and the alkaloids were extracted with 350 ml of chloroform. Chloroform was evaporated under vacuum conditions and the dried extracts were dissolved in methanol at 1 mg/ml for analysis by capillary gas chromatography-mass spectrometry (GC/MS), and 2–4 mg/ml for bioactivity analysis.

Alkaloid isolation and identification
Pure alkaloids were obtained from different plants. From bulbs of *Z. carinata*, 6 alkaloids were obtained as follows: 1.8 kg of dried and ground bulbs were exhaustively extracted with methanol. The solvent was evaporated and the residues were dissolved in 2% sulphuric acid and defatted with ethyl acetate. Subsequently, the aqueous layers were basified with 25% ammonia up to a pH of 9.5–10.0, and the alkaloids were extracted with chloroform. After the extraction, 6 g of the 7.92 g of alkaloid extract was purified using silica gel CC (CHCl$_3$-MeOH), from 90 : 10 to 0 : 100, and nine fractions were obtained (Fr. 1–9). Using Sephadex LH-20 CC (MeOH), Fr. 4 (660 mg) was separated and seven fractions were collected (Fr. 4A–Fr. 4G). The subfraction 4A was again fractionated, yielding criasbetaine (31.9 mg). The fractionation of subfraction 4D yielded lycorine (2.3 mg) and pseudolycorine (4.6 mg). Separation of Fr. 5 (42 mg) allows epivittatine (1.7 mg) to be obtained. Ten fractions were obtained from Fr. 7 (510 mg) (7A–7J), and lycoramine (20.6 mg) was identified in 7B. Subfraction 7J was separated by semi-preparative RPC18 HPLC (H$_2$O-ACN-MeOH-TFA, 80 : 10 : 10 : 0.01) to yield the compound vittatine (5.4 mg, Rt 8.00 min). The purified *Z. carinata* alkaloids were identified by comparing NMR spectroscopic data with those previously reported in the literature, as well as from their GC/MS fragmentation patterns and comparison with commercial and private databases (methodology described in the next section). On the other hand, ismine, 3-epimacronine, and tazettine were isolated from *Worsleya procera* as described previously (Gonring-Salarini et al., 2019). Albomaculine, aulicine, and trisphaeridine were isolated from *Hippeastrum aulicum* (Bessa et al., 2017). 7-deoxy-*trans*-dihydronarciclasine was isolated from *Hippeastrum goianum* (Lianza et al., 2020). Hippeastrine, candimine, and 2α,7-dimethoxyhomolycorine were isolated from two unidentified Brazilian species of the *Hippeastrum* genus.

GC-MS analysis

The GC-MS analyses were carried out on a GC-MS 7890 system (Agilent, USA), operating in EI mode at 70 eV, and using an HP-1 MS capillary column (30 m × 0.25 mm × 0.25 μm). The temperature program was as follows: 1 min held at 120 ºC, 120–210 ºC at 15 ºC min^{-1}, 210–260 at 8 ºC min^{-1}, and 260–300 ºC at 15 ºC min^{-1}. The injector temperature was 280 ºC in splitless mode. One microliter of the solution was injected. The alkaloids were identified by comparing their mass spectral fragmentation with standard reference spectra from the NIST database (NIST Mass Spectral Database, National Institute of Standardization and Technology, USA) and a library dedicated exclusively to AA. Mass spectra were deconvoluted using AMDIS 2.64 software (NIST). The proportion of each individual compound in the alkaloid fractions was expressed as a percentage of the total alkaloid mass.

Bioactivity evaluation

Cell culture

The human keratinocyte cell line HaCaT, supplied by the San Vicente de Paul Hospital Cell Bank (Medellín-Colombia), was maintained in Dulbecco's Modified Eagle's Medium, supplemented with 10% fetal bovine serum and 1% of an antibiotics mixture (60 μg/ml penicillin and 100 μg/ml streptomycin), at 37 °C in a humidified 5% CO_2 incubator. The maximum passage used in experiments with HaCaT cell line was 23. The human melanoma cell line VMM18 (ATCC® CRL3229™) was grown in RPMI 1640, supplemented with 10% fetal bovine serum, and 1% of an antibiotics mixture (60 μg/ml penicillin and 100 μg/ml streptomycin), at 37 °C in a humidified 5% CO_2 incubator. The maximum passage used in experiments with VMM18 cell line was 8. The ingredients of the complete cell culture media, the fetal bovine serum and antibiotics were purchased from Gibco®.

Cell viability assays

HaCaT keratinocytes and VMM18 melanoma cells were seeded at 3000 and 5000 cells/well, respectively, in 96-well plates and left overnight to adhere. The cells were then treated with six concentrations (1.25–80.0 μg/ml) of alkaloid fractions and alkaloids for 24 h. Cell viability was analyzed by a CCK-8 assay using a WST-8 tetrazolium salt (Dojindo Molecular Technologies, Inc.), according to the manufacturer's instructions.

Measurement of intracellular ROS

HaCaT cells ($5 × 10^4$ cell per well) were seeded in 96-well plates with the supplemented medium overnight at 37 °C in 5% CO_2. The medium was removed, and the cells were treated with the extracts (2.5, 5.0 and 10.0 μg/ml) for 24 h. Next, the cells were washed with PBS, and after adding 100 μl of 2',7-dichlorodihydrofluorescein-diacetate (H_2DCFDA, 25 μM) to each well, incubated for 30 min at 37 °C in 5% CO_2. Subsequently, the cultured cells were irradiated with 100 mj/cm^2 UVB (312 nm) and incubated for 15 min. The intracellular ROS were measured as DCF fluorescence at 485–516 nm ex/em, using a Synergy HT Multi-mode-microplate reader at 37 °C. Quercetin was used for the control assay.

Modulation of the inflammation biomarkers

HaCaT cells ($1 × 10^6$ cells/well) were seeded in six-well plates. After 24 h, the cells were irradiated with 60 mj/cm^2 of UVB light at 312 nm and incubated for 6 h at 37 °C in a 5% CO_2 atmosphere. After treatment, the cell lysates and supernatant were collected to measure the IL-6 levels using ELISA kits (R&D systems), according to the manufacturer's instructions. The biomarker level was determined based on an absorbance of 450 nm, measured using a BioTek plate reader.

Oxygen radical absorbance capacity (ORAC) assay

The hydrophilic ORAC assay was adapted from previously described procedures (Duque et al., 2017). First, 50 μl of sample solution or Trolox standard was mixed with 150 μl of fluorescein (1.6 μm) and incubated at 37 °C for 30 min. After which, 50 μl of AAPH (2,2'-Azobis(2-amidinopropane) dihydrochloride) solution (125 mm) was added. Fluorescence was measured every 2 min for 120 min at an excitation wavelength of 485 nm and an emission wavelength of 520 nm, using a Synergy HT Multi-mode-microplate reader (Biotek Instruments, Inc.; Winooski, USA). The relative ORAC values were expressed as micromol Trolox equivalent per gram of alkaloid fraction (μmol TE/g AF).

Statistical analysis

In vitro experiments were evaluated using at least three independent assays. Data with homogenous variance were analyzed by ANOVA using PRISM software. The statistical significance of the differences between controls and samples was determined using Dunnet's multiple comparison test ($p < 0.05$ (*) significant, $p < 0.01$ (**) very significant, $p < 0.001$ (***) extremely significant). Bonferroni's multiple comparison test was used to determine the statistical significance of the differences within each sample. Error bars on graphs represent standard deviation (SD).

Chemometric analysis

To link the chemical profiles with the biological activities of the alkaloid fractions, a chemometric analysis was performed. The spectral data matrix obtained from AMDIS 2.64 software, including m/z, retention time, and peak area for each detected ion, was imported into Excel Microsoft Office 2011 version 14.7.7 (2010 Microsoft Corporation) and merged with the bioactivity dataset (cell viability, ROS production and IL-6 production) to form the final matrix. All statistical models used – namely principal component analysis and partial least squares regression – were computed using the open source software R-project 3.1.0 (RStudio, Inc) and the following packages: "mdatools" (Kucheryavskiy, 2021), "REdaS" (Maier, 2015) and "pls" (Mevik et al., 2019).

Results

Chemical analysis by GC-MS and purification of alkaloids

GC-MS was used for the detection, identification, and quantification of AA from the bulbs and leaves of four Amaryllidaceae species. 24 alkaloids were detected, 14 of them identified from their mass spectra (Table 1). Narciclasine, haemanthamine, lycorine, galanthamine, tazettine, and crinine were the main structural types found (Berkov et al., 2020). On the other hand, the dried bulbs of *Z. carinata* were extracted and purified as previously described, leading to the isolation and identification of 6 known alkaloids by their NMR spectroscopic data and GC/MS fragmentation patterns. Other AA were also evaluated to investigate their photoprotective and anti-cancer properties (Fig. 1).

Table 1. Composition of the alkaloid fractions of four Amaryllidaceae plants

Ítem †	Alkaloid	Type	M+	Ions (% Intensity)	t$_r$(min)	PERCENTAGES OF RELATIVE PEAK AREA ††						
						C. jagus (B)	C. jagus (L)	H. elegans (B)	H. elegans (L)	Z. carinata (B)	Z. carinata (L)	E. caucana (B)
1	M+ 156	–	156 (2)	154 (20), 125 (18), 120 (100), 107 (34), 77 (21), 70 (31)	7.6	1%	11%		10%			
2	M+ 155	–	155 (7)	154 (100), 125 (43), 86 (22), 70 (95)	8.4		4%					
3	Ismine	Ismine	257 (5)	238 (36), 223 (100), 138 (50), 111 (30)	13.7	20%	9%			13%	11%	8%
4	5,6-Dihydrobicolorine	Ismine	239 (42)	238 (100), 180 (11), 118 (9), 90 (10)	15.0	3%	2%			3%	2%	2%
5	Epigalanthamine	Galanthamine	287 (78)	270 (14), 244 (24), 216 (36), 174 (35), 115 (18)	17.0					3%	3%	
6	Lycoramine	Galanthamine	289 (57)	288 (100)	17.7			80%	59%	28%	22%	
7	O-Demethyllycoramine	Galanthamine	275 (50)	274 (100), 256 (7), 188 (14), 181 (9), 173 (26), 115 (28), 77(21), 51 (9)	18.3			20%	31%			
8	Vitattine	Haemanthamine	271 (100)	252 (26), 228 (24), 199 (79), 187 (71), 129 (25), 115 (35)	19.4	51%	2%			13%	22%	8%
9	M+ 251		251 (43)	250 (100), 192 (12), 124 (9), 95 (12)	20.3		2%					
10	8-O-Demethylmaritidine	Haemanthamine	273 (97)	256 (20), 230 (26), 201 (100), 189 (53), 175 (22), 115 (41), 91 (23), 77 (24), 56 (34)	20.8					6%		1%
11	Cherylline	–	285 (20)	242 (63), 241 (60), 225 (100), 211 (46), 198 (15), 182 (12), 165 (16)	24.0	3%	2%					
12	11,12 dehydroanhydrolycorine	Lycorine	249 (57)	248 (100), 190 (25), 95 (20)	24.7	1%				4%	6%	8%
13	Buphanidrine	Crinine	315 (100)	300 (31), 284 (36), 260 (38), 245 (64), 231 (24), 215 (20), 202 (22), 130 (29), 115 (24)	27.3		32%					
14	M+ 319	–	319 (100)	304 (21), 288 (40), 272 (70), 261 (29), 233 (79), 218 (27), 128 (19), 91 (20)	27.2					4%	6%	
15	Tazettine	Tazettine	331 (23)	316 (12), 298 (18), 247 (100), 227 (12), 201 (18), 181 (16), 115 (16), 70 (31)	28.3					7%	3%	73%
16	M+ 269	–	269 (100)	240 (35), 225 (18), 211 (21), 181 (70), 153 (18), 115 (16)	27.5	2%				7%	8%	
17	Powelline	Crinine	301 (100)	300 (11), 282 (182), 258 (23), 229 (92), 217 (55), 203 (22), 115 (30), 77 (18), 56 (20)	28.7	18%	8%					
18	Galanthine	Lycorine	317 (19)	298 (8), 268 (14), 243 (90), 242 (100), 162 (10), 125 (11)	30.2					7%		
19	Lycorine	Lycorine	287 (22)	268 (19), 250 (22), 227 (62), 226 (100)	30.4					5%		
20	Undulatine	Crinine	331 (100)	286 (16), 258 (33), 217 (30), 205 (65), 189 (40), 173 (33), 145 (13), 115 (25)	31.3		17%					
21	M+ 297	–	297 (52)	296 (100), 280 (18), 148 (11)	32.3						9%	
22	M+ 319	–	319 (100)	302 (11), 275 (34), 246 (22), 232 (70), 220 (31), 219 (26), 191 (16), 115 (17), 77 (18)	33.2	2%	11%					
23	M+ 295	–	295 (85)	294 (100), 278 (12), 147 (11)	34.5						7%	
24	Oxoassoanine	Lycorine	281 (97)	280 (36), 266 (11), 250 (14), 140 (14), 94 (100)	35.3					1%		
	DETECTED ALKALOIDS					9	11	2	3	13	11	6

† Peak numbering of signals in the chromatogram. †† Percentage of the alkaloid relative to the total alkaloid content.
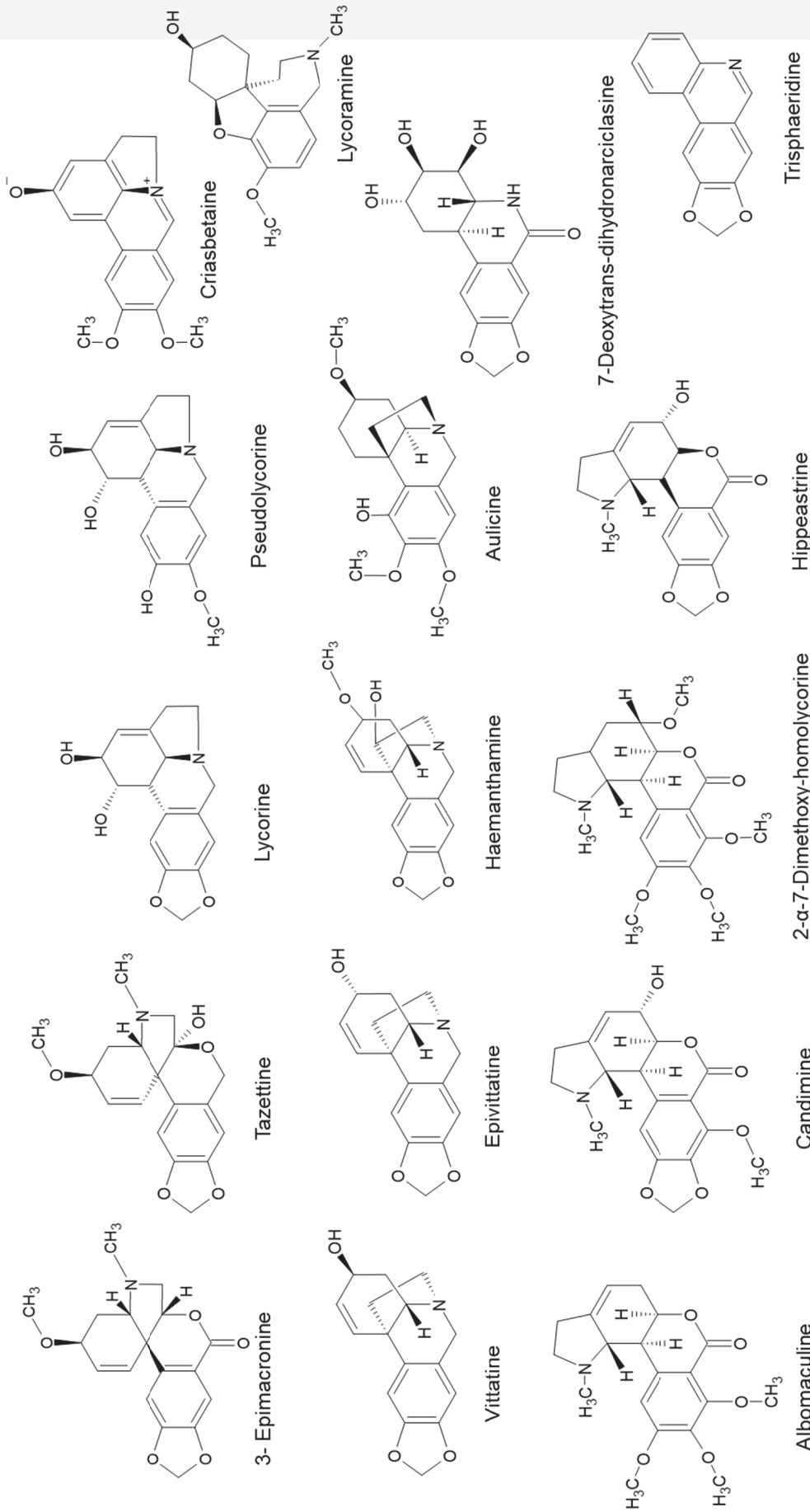
Fig. 1. Chemical structure of evaluated Amaryllidaceae alkaloids

Effect of alkaloid fractions and isolated alkaloids on the viability of human keratinocyte cells

Seven alkaloid fractions and sixteen alkaloids were evaluated for their effect on the viability of HaCaT cells. In general, the alkaloid fractions did not cause significant changes in cell viability, and the degrees of toxicity were dose dependent. The fractions from *C. jagus, E. caucana, H. elegans*, and *Z. carinata* bulbs significantly reduced cell viability at several concentrations (40–100 μg/ml), whereas those from leaves reduced cell viability only at the highest tested concentration (100 μg/ml). Thus, the alkaloid fractions from bulbs exhibited higher cytotoxicity than those from leaves. In contrast, alkaloid fractions from *C. jagus* leaves significantly increased cell viability at 10–40 μg/ml (Fig. 2A). Among the pure alkaloids, aulicine, criasbetaine, epivittatine, lycoramine, pseudolycorine, trisphaeridine and vittatine reduced HaCaT cell viability at low concentrations (1.25–20 μg/ml), whereas 3-epimacronine was found to be non-cytotoxic. A significant decrease in cell viability was induced by haemanthamine, 7-deoxy-*trans*-dihydronarciclasine, 2α,7-dimethoxyhomolycorine and lycorine at all tested concentrations, in a concentration-dependent manner (Fig. 2B). These alkaloids were therefore determined to be cytotoxic. Dacarbazine was used as a reference drug in the experiments.
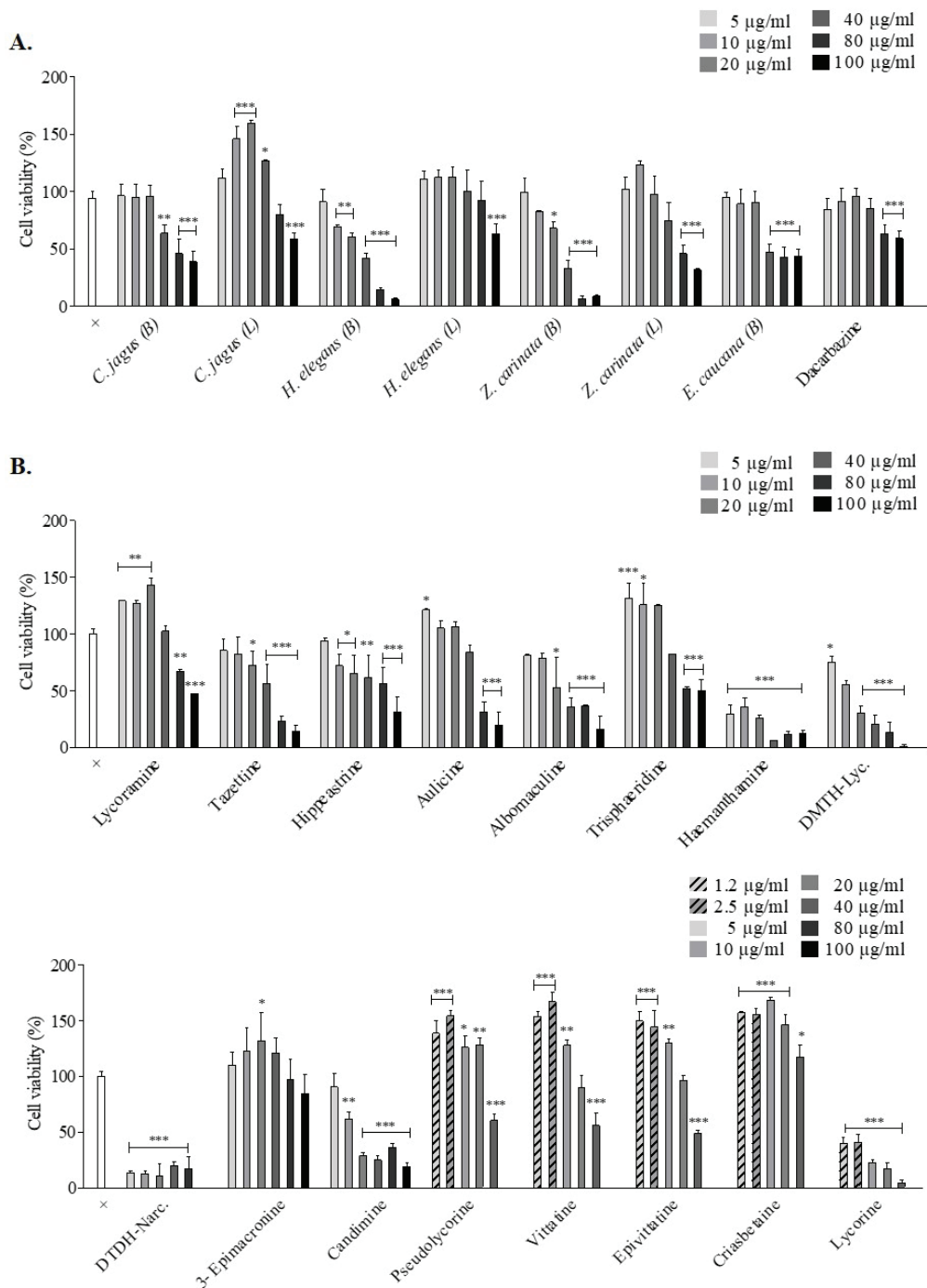

Fig. 2. Effect on cell viability and proliferation of human keratinocytes (HaCaT cells). (**A**) Effect of alkaloid fractions. (**B**) Effect of isolated alkaloids. (x): Untreated cells. Significance level of differences between samples and (x) are indicated with: * Significant (*p* < 0.05); ** Very significant (*p* < 0.01); and *** Extremely significant (*p* < 0.001) (Dunnett's test).

Photoprotective effects of alkaloid fractions and isolated alkaloids on UVB-irradiated human keratinocyte cells

Subsequent experiments were performed using concentrations of 1.25–10.0 μg/ml, as no toxic effects were observed at this range. After 24 hours of treating HaCaT cells with the alkaloid fractions and pure alkaloids, followed by exposure to a non-toxic UVB dose (100 mj/cm^2), no reduction in cell viability was observed (data not show), but ROS generation was 10-fold higher in the positive control than in the cells that were untreated and non-UVB-exposed. As shown in Fig. 3A, all alkaloid fractions tested, except for *C. jagus* (L), reduced ROS levels by 20–30% in comparison with untreated UVB-irradiated cells. The *E. caucana* (B) fraction at 2.5 μg/ml offered the most protection from UVB-induced oxidative stress (31.6%). With respect to the pure alkaloids, non-toxic compounds were chosen for photoprotective activity or cytotoxic test on melanoma cells, based on preliminary data. Tazettine at 2.5 μg/ml had the highest protective effect (29.4%), comparable with that of quercetin (reference compound). Lycoramine and hippeastrine also significantly reduced intracellular ROS at 5.0 μg/ml. The other evaluated alkaloids were found to be inactive (Fig. 3B). To determine if the alkaloid fractions and pure alkaloids inhibited UVB-induced ROS production via an

antioxidant mechanism, hydrogen atom transfer (HAT) reactions in an ORAC assay were carried out, using quercetine as a reference. Pseudolycorine and aulicine showed the highest antioxidant activity, followed by *C. jagus* (L) and *H. elegans* (B) fractions and tazettine. In general, alkaloid fractions produced higher ORAC values than pure alkaloids (Fig. S1).

To examine the inhibitory effect of the alkaloid fractions and alkaloids on IL-6 production, HaCaT cells were irradiated with UVB light (60 mj/cm^2) for 6 hours and then treated with different concentrations of the extracts. In this assay, the positive control exhibited a significantly higher IL-6 production than the untreated and non-UVB-exposed cells. Dexamethasone was used as a reference anti-inflammatory drug, and its modulatory effect was observed at 5.0–10.0 μg/ml. The *Z. carinata* (B) fraction showed the highest bioactivity, reducing IL-6 intracellular production by 90.8% ($p < 0.001$) at 10.0 μg/ml. In addition, *H. elegans* (B), *Z. carinata* (L), *E. caucana* (B) fractions at 10 μg/ml reduced the biomarker by 41%, 44%, and 49%, respectively, compared to the positive control. In general, bioactive alkaloid fractions were more potent than dexamethasone. In contrast, the *C. jagus* (L) fraction increased IL-6 production at 5.0 μg/ml, but no effect was observed at the other tested concentrations (Fig. 3C). Among the pure alkaloids, lycoramine was the most potent, reducing IL-6 production by 70.4% at 2.5 μg/ml (Fig. 3D).
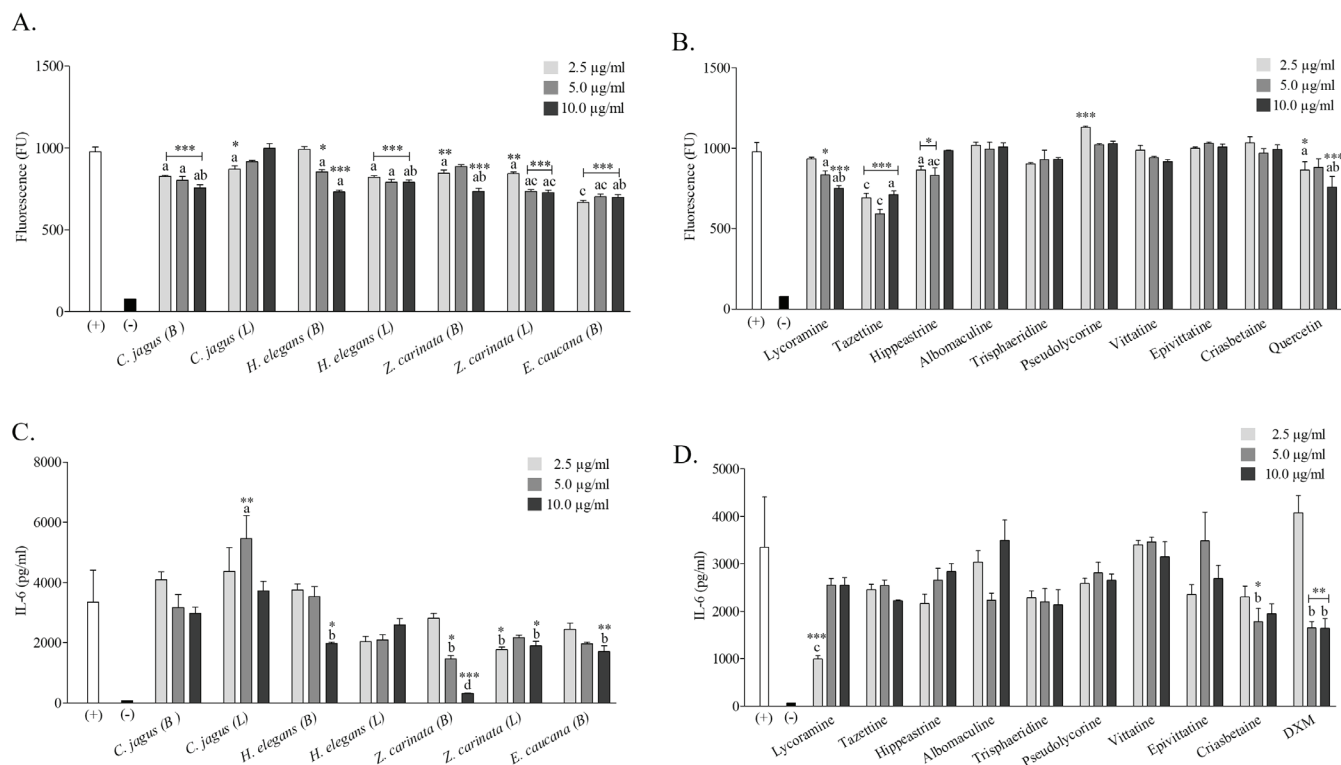

Fig. 3. Photoprotective effects on UVB-irradiated human keratinocyte cells. (**A**) Effect of alkaloid fractions on UVB-induced intracellular ROS production. (**B**) Effect of isolated alkaloids on UVB-induced intracellular ROS production. (**C**) Effect of alkaloid fractions on UVB-induced intracellular IL-6 production. (**D**) Effect of isolated alkaloids on UVB-induced intracellular IL-6 production. (+) Positive control: untreated and UVB-exposed cells. (−) Negative control: untreated and non-UVB-exposed cells. DXM: Dexamethasone. Different letters mean significant differences between samples. (Bonferroni test, $p < 0.05$). Significance level of differences between samples and (+) are indicated with: * Significant ($p < 0.05$); ** Very significant ($p < 0.01$); and *** Extremely significant ($p < 0.001$) (Dunnett's test).

Cytotoxic effects of alkaloid fractions and isolated alkaloids on melanoma cells

The cell viability and proliferation induced by alkaloid fractions and pure alkaloids was evaluated in the human melanoma VMM18 cell line. The *E. caucana* (B) fraction was the most cytotoxic, reducing cell viability by 45.7% at 20 µg/ml, an effect not statistically different from that of dacarbazine, which reduced the cell viability by 48.9% at the same concentration

(Fig. 4A). On the other hand, 7-deoxy-*trans*-dihydronarciclasine exhibited cytotoxic activity against melanoma cells at all tested concentrations, whereas hippeastrine, tazettine, and trisphaeridine significantly reduced cell viability at over 40 µg/ml. The other alkaloidal fractions and pure alkaloids showed non-significant cytotoxicity below 80.0 µg/ml against melanoma cells (Fig. 4B).
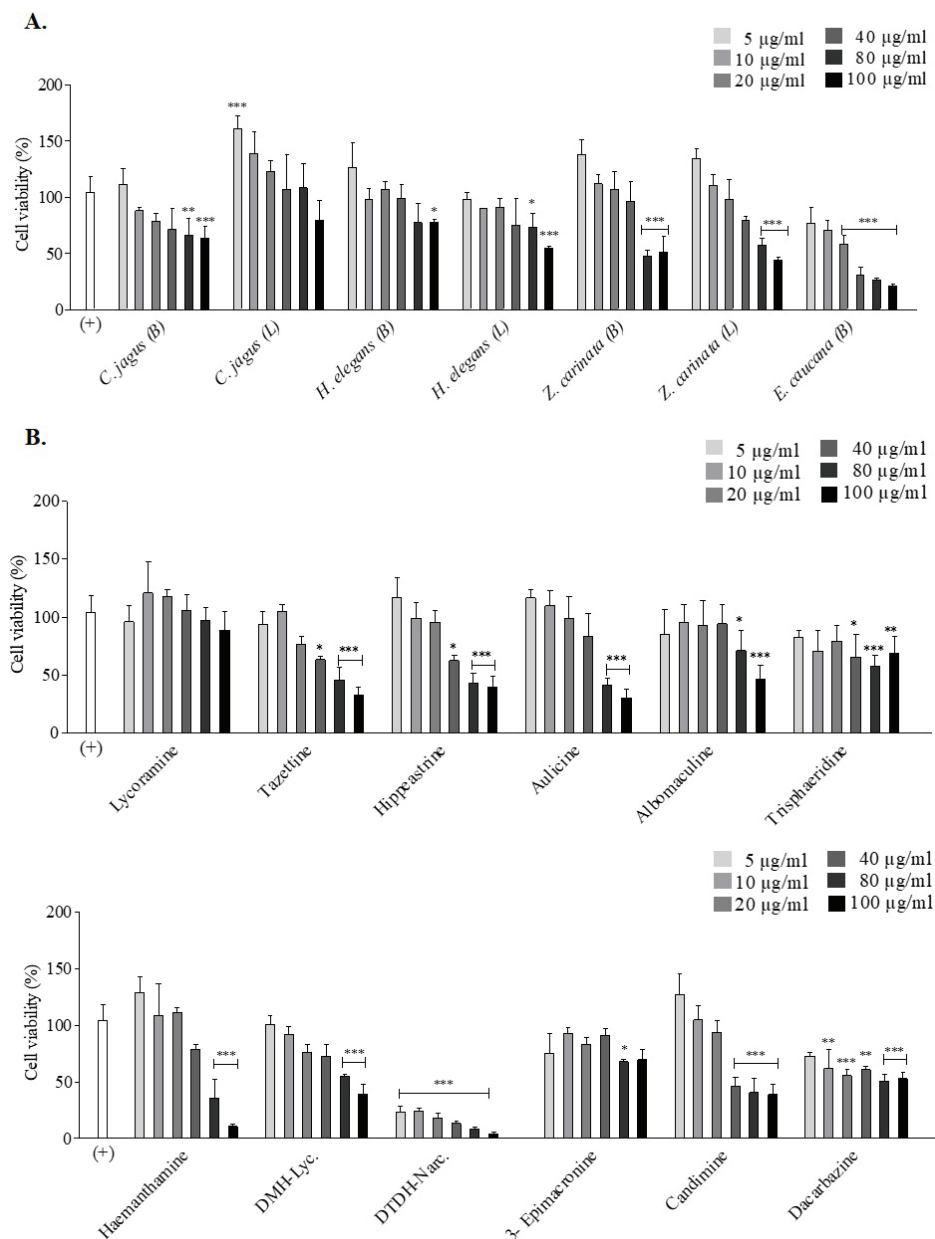

Fig. 4. Cytotoxic effects on melanoma VMM18 cell line. (**A**) Effect of alkaloid fractions. (**B**) Effect of isolated alkaloids. (+): Positive control, untreated cells. Significance level of differences between samples and (+) are indicated with: * Significant ($p < 0.05$); ** Very significant ($p < 0.01$); and *** Extremely significant ($p < 0.001$) (Dunnett's test).

Multivariate analysis

Most of the identified chemical variables were associated with *Z. carinata* fractions due to their rich composition. *C. jagus* fractions were characterized by the presence of cherylline, powelline, and undulatine alkaloids; *H. elegans* fractions by lycoramine and O-demethyllycoramine, and *E. caucana* (B) fractions by tazettine (Fig. S2A). In addition, four regression models were constructed: (1) the viability of keratinocytes; (2) cytotoxicity against melanoma cells; (3) intracellular ROS production; (4) IL-6 production in keratinocytes exposed to UVB radiation. Red-labeled signals indicate chemical variables (Table 1) which positively affect the model; that is, alkaloids that increase each biological variable. Whereas blue variables indicate the alkaloids that contribute to the negative behavior of the model. The regression model built for keratinocyte cytotoxicity showed an $R^2 = 0.9984$, and the highest coefficient regression was assigned to lycoramine (X6), 8-*O*-demethylmaritidine (X10), tazettine (X15), galanthine (X18), and lycorine (X19). The regression model for melanoma cell cytotoxicity exhibited an $R^2 = 0.9443$, and determined vittatine (X8) and tazettine (X15) as variables with the highest statistical significance (Fig. S2B). On the other hand, in the regression model for intracellular ROS production, $R^2 = 1.0000$, and the highest statistical weight was assigned to lycoramine (X6), vittatine (X8), and tazettine (X15). Whereas for IL-6 production, $R^2 = 0.6379$, and lycoramine (X6), tazettine (X15), X16, and galanthine (X18) were identified as the most important chemical variables in biological activity (Fig. S2C).

Discussion

In the field of photocarcinogenesis, UVB-mediated oxidative stress and inflammation represent the most important molecular mechanisms, as ROS overproduction damages cell structures and ROS act as secondary messengers in key signaling pathways, such as MAPK. Furthermore, pro-inflammatory cytokines trigger mechanisms related to tumor growth, such as epidermal hyperplasia and infiltration of leukocytes (Afaq, 2011; Atanasov et al., 2021; Nichols and Katiyar, 2010). This study evaluated the therapeutic potential of AA in skin cancer by testing their anti-proliferative activity in melanoma cells and photoprotective effects in normal keratinocytes exposed to UVB radiation. The capacity to modulate ROS and IL-6 production was also determined.

The results are consistent with previous data on the cytotoxicity of some AA types. Lycorine, the first alkaloid to be isolated from the Amaryllidaceae plants, has been studied for its antiproliferative activity and found to reduce the growth of a wide variety of tumor cells *in vivo* and *in vitro*. Its effects have been related to a capacity to form a complex with tRNA, which inhibits protein synthesis by preventing the binding of amino acids to the ribosome (Nair et al., 2016b). Other studies have reported the cytotoxic activity of lycorine in leukemia cells, bladder and breast cancer, and a large number of other cell lines (Dasari et al., 2014; Wang et al., 2016; Ying et al., 2017). The results obtained in the present study suggest that the reduction in HaCaT cell viability caused by lycorine may be closely related to the methylenedioxy ring located between C8 and C9 (Cao et al., 2013; Nair et al., 2016a), as pseudolycorine and criasbetaine, which possess the same lycorine skeleton but with methoxy and hydroxyl substituents at C8 and C9 (Fig. 1), showed a contrary effect by significantly increasing viability.

Haemanthamine is also reported to have antiproliferative activity in different types of human tumor cells, such as lymphoma, leukemia, hepatoma, cervix, and prostate. Its mechanism is related to ribosome 60S subunit binding and the blocking of protein synthesis (Nair et al., 2012). In HaCaT cells, we observed it has a greater cytotoxic activity than vittatine and epivittatine (>40 μg/ml). It is possible that the hydroxyl and/or methoxy substituents at C11 and C3 of haemanthamine increase the cytotoxicity of this alkaloid type against keratinocytes. Narciclasine, on the other hand, is a recognized regulator of plant cell growth with cytotoxic properties (Berkov et al., 2020; Nair et al., 2016a). Narciclasine-type alkaloids are known to have a potent antitumor effect on apoptosis-resistant cells associated with blocking the assembly of the actin cytoskeleton (Ingrassia et al., 2009; Kornienko and Evidente, 2008), a mechanism that may underlie the toxicity of 7-deoxy-*trans*-dihydroarciclasine. Additionally, the biological activity of homolycorine-type alkaloids, recognized for their antiviral and analgesic properties, has been less studied (Bastida et al., 2006; Masi et al., 2019). The results of the present study suggest that this alkaloid type has cytotoxic effects in the HaCaT model, as hippeastrine, albomaculine, and candimine (all homolycorine-type alkaloids) significantly reduced cell viability at 10 μg/ml.

Most of the tested samples showed moderate cytotoxicity against melanoma cells, except *H. elegans* (B) and *E. caucana* (B) alkaloid fractions, and tazettine and trisphaeridine, which were highly potent. Interestingly, only the *E. caucana* (B) alkaloid fraction at 20 μg/ml significantly reduced the viability of melanoma cells without affecting healthy keratinocytes. Its effect was not significantly different from that of dacarbazine.

The improved viability of HaCaT cells induced by some of the extracts may be associated with cytotoxic mechanisms, as hyperproliferative states of keratinocytes can occur during pathological processes, such as psoriasis and malignant hyperplasia (Lee et al., 2002). For instance, the effect of the *C. jagus* (L) alkaloid fraction, which induced an increase in keratinocyte viability, could be related to the production of inflammatory cytokines (Chorachoo et al., 2016; Lee et al., 2020; Qiao et al., 2019). In fact, this extract significantly increased IL-6 production in keratinocytes compared to the positive control at 10 μg/ml (Fig. 3). Recently, IL-6 has been reported as a marker of a pathological process in psoriasis (Muramatsu et al., 2016). Furthermore, hyperproliferative effects of pseudolycorine at 2.5 μg/ml in HaCaT cells could be associated with the increase in ROS production (Fig. 3), since free radical oxidation of proteins activate the MAPK pathway, which in turn activates the transcription factor AP-1 and leads to cell proliferation stimuli (Montes de Oca et al., 2017).

The non-cytotoxic extracts were tested for their photoprotective potential at <10 μg/ml in HaCaT cells. Alkaloid fractions had greater antioxidant effects than pure alkaloids (Fig. S1), with the single exception of the *C. jagus* (L) alkaloid fraction at high concentrations. The latter effect could be explained by the presence of oxidant compounds such as buphanidrine (X12) (Table 1), identified by the PLS-R analysis as a variable that increases intracellular ROS production (Fig. 3B). On the other hand, the reduction in intracellular ROS induced by lycoramine, tazettine, and hippeastrine could be due to their capacity to modulate endogenous antioxidant mechanisms related to peroxide production (H_2O_2), considering that the H_2DCFDA assay mainly identifies this type of ROS (Wu and Yotnda, 2011). However, this activity could also be explained by a free radical stabilizing capacity. Lycoramine and tazettine possess one O-H group close to two electrons of the N that stabilize the O generated after reaction with the free radical (Cortes et al., 2018). In addition, the enol group

of hippeastrine can stabilize free radicals formed from the homolytic cleavage of the O-H group in C2, a mechanism reported for galanthamine antioxidant activity (Traykova et al., 2003). In contrast, pseudolycorine at 2.5 µg/ml increased ROS production (1.15-fold) compared to the positive control; a negative effect that enhances oxidative stress and could be related to the hyperproliferative activity observed in HaCaT cells (Fig. 2B), considering that oxidative stress triggers proliferation pathways such as NF-κB, AP-1 and MAPK (Reuter et al., 2010). Spearman and Pearson ratio coefficients between ORAC values and intracellular ROS reduction were –0.22 and –0.97, respectively, indicating that an increase in the ORAC value is weakly related to the decrease in ROS production. This suggests that despite their chemical structure, alkaloids can reduce oxidative stress, mainly by interacting with different signaling pathways. In addition, we partially validated the results of the PLS-R analysis by confirming that lycoramine (X6) and tazettine (X15) effectively protected cells from UVB-induced oxidative stress (Fig. 3B).

The production of ROS and IL-6 in keratinocytes exposed to UVB radiation was significantly reduced by lycoramine, *Z. carinata* (B and L), and *E. caucana* (B). Furthermore, correlation profiles of PLS-R analysis matching ROS and IL-6 reduction suggest that these parameters are similarly affected by common chemical variables. Lycoramine (X6) and tazettine (X15) had a photoprotective effect, reducing ROS and IL-6 production, whereas *O*-demethylycoramine (X7), buphanidrine (X13), powelline (X17), and undulatine (X20) enhanced both biomarkers (Fig. S2). These findings support the interdependence between oxidative stress and inflammation previously described in carcinogenesis (Biswas, 2016; Reuter et al., 2010). Moreover, the lower intracellular IL-6 production induced by lycoramine (X6) partially validates the results of the PLS-R analysis, although this was not the case for other alkaloids.

The chemometric analysis also suggested that cytotoxic effects of alkaloid fractions on HaCaT cells were due to lycoramine (X6), 8-*O*-demethylmaritidine (X10), tazettine (X15), galanthine (X18), and lycorine. These results were validated by the bioactivities shown by some of the pure alkaloids, namely lycoramine, tazettine, and lycorine – which were cytotoxic at 80, 20, and 1.25 µg/ml, respectively (Fig. 2). On the other hand, the results of the multivariate analysis of the cytotoxic activity of extracts in melanoma cells were partially validated by the observation of tazettine cytotoxicity at 40 µg/ml (Fig. 4B). However, this bioactivity could not be tested for vittatine in our study. In summary, the *E. caucana* (B) alkaloid fraction exhibited the highest potential as an antitumoral agent due to its selective cytotoxicity in cancer cells at a low concentration (20 µg/ml) (Fig. S3). This result could be explained by the synergistic effect of alkaloids found in this extract. Previous studies have proposed the use of multi-agent therapies to enhance cancer treatment outcomes (Bhatt et al., 2020; Bolton et al., 2019). In such a strategy, one drug has a toxic effect on tumor cells and promotes a phenotypic adaptation that leaves cells more vulnerable to a second agent, thereby maintaining a longer-lasting tumor control (Cunningham et al., 2011).

Conclusions

These results provide the first evidence of the chemotherapeutic and photoprotective potential of AA in skin cancer. The *E. caucana* (B) alkaloid fraction exhibited cytotoxic activity against melanoma cells and a capacity to modulate UVB-induced oxidative stress and inflammation biomarkers in healthy keratinocytes. The fact that this fraction matched the activity of dacarbazine suggests it has pharmacological potential in an anticancer multi-agent strategy. This study has also revealed the photoprotective potential of lycoramine and tazettine, which protected human keratinocytes from UVB-induced production of ROS and IL-6. Overall, the alkaloid fractions were more effective than the pure alkaloids, and the *Z. carinata* (B) alkaloid fraction showed the highest potential as an anti-inflammatory agent. Our findings confirm that the multi-agent composition of natural extracts could increase the effectiveness of chemotherapeutic and photoprotective strategies; with the best option being a mixture of alkaloids – preferably with defined concentrations. Overall, this study has contributed to the search for new anticancer and photoprotective molecules through the establishment of an experimental model that allows pre-clinical evaluation of the therapeutic and preventive potential of natural molecules in skin cancer.

Ethical aspects and conflict of interests
The authors have no conflict of interests to declare.

Author contributions
CC, KB, and EO designed the study. CC, KB, NC, and JB developed the biological tests. NC, WB, and JB carried out phytochemical studies or provided molecules. CC performed sample processing and analysis. CC, KB, EO analyzed the data and wrote the manuscript. All authors critically revised the manuscript.

References

Afaq F (2011). Natural agents: Cellular and molecular mechanisms of photoprotection. Arch Biochem Biophys 508(2): 144–151. DOI: 10.1016/j.abb.2010.12.007.

Apalla Z, Lallas A, Sotiriou E, Lazaridou E, Ioannides D (2017b). Epidemiological trends in skin cancer. Dermatol Pract Concept 7(2): 1–6. DOI: 10.5826/dpc.0702a01.

Apalla Z, Nashan D, Weller RB, Castellsagué X (2017a). Skin cancer: Epidemiology, disease burden, pathophysiology, diagnosis, and therapeutic approaches. Dermatol Ther (Heidelb) 7(Suppl. 1): 5–19. DOI: 10.1007/s13555-016-0165-y.

Atanasov AG, Zotchev SB, Dirsch VM, International Natural Product Sciences Taskforce, Supuran CT (2021). Natural products in drug discovery: advances and opportunities. Nat Rev Drug Discov 20(3): 200–216. DOI: 10.1038/s41573-020-00114-z.

Bastida J, Lavilla R, Viladomat F (2006). Chapter 3 Chemical and Biological Aspects of Narcissus Alkaloids. Alkaloids Chem Biol 63: 87–179. DOI: 10.1016/s1099-4831(06)63003-4.

Berkov S, Osorio E, Viladomat F, Bastida J (2020). Chemodiversity, chemotaxonomy and chemoecology of Amaryllidaceae alkaloids. Alkaloids Chem Biol 83: 113–185. DOI: 10.1016/bs.alkal.2019.10.002.

Bessa CDPB, de Andrade JP, de Oliveira RS, Domingos E, Santos H, Romão W, et al. (2017). Identification of alkaloids from *Hippeastrum aulicum* (Ker Gawl.) Herb. (Amaryllidaceae) using CGC-MS and ambient ionization mass spectrometry (PS-MS and LS-MS). J Braz Chem Soc 28(5): 819–830. DOI: 10.21577/0103-5053.20160234.

Bhatt VR, Shostrom V, Holstein SA, Al-Kadhimi ZS, Maness LJ, Berger A, et al. (2020). Survival of older adults with newly diagnosed acute myeloid leukemia: Effect of using multiagent versus single-agent chemotherapy. Clin Lymphoma Myeloma Leuk 20(5): e239–e258. DOI: 10.1016/j.clml.2020.01.015.

Biswas SK (2016). Does the interdependence between oxidative stress and inflammation explain the antioxidant paradox?. Oxid Med Cell Longev 2016: 5698931. DOI: 10.1155/2016/5698931.

Bolton NM, Maerz AH, Brown RE, Bansal M, Bolton JS, Conway WC (2019). Multiagent neoadjuvant chemotherapy and tumor response are associated with improved survival in pancreatic cancer. Hpb (Oxford) 21(4): 413–418. DOI: 10.1016/j.hpb.2018.08.013.

Cao Z, Yu D, Fu S, Zhang G, Pan Y, Bao M, et al. (2013). Lycorine hydrochloride selectively inhibits human ovarian cancer cell proliferation and tumor neovascularization with very low toxicity. Toxicol Lett 218(2): 174–185. DOI: 10.1016/j.toxlet.2013.01.018.

Chorachoo J, Saeloh D, Srichana T, Amnuaikit T, Musthafa KS, Sretrirutchai S, Voravuthikunchai SP (2016). Rhodomyrtone as a potential anti-proliferative and apoptosis inducing agent in HaCaT keratinocyte cells. Eur J Pharmacol 772: 144–151. DOI: 10.1016/j.ejphar.2015.12.005.

Cortes N, Castañeda C, Osorio EH, Cardona-Gomez GP, Osorio E (2018). Amaryllidaceae alkaloids as agents with protective effects against oxidative neural cell injury. Life Sci 203: 54–65. DOI: 10.1016/j.lfs.2018.04.026.

Cragg GM, Pezzuto JM (2016). Natural products as a vital source for the discovery of cancer chemotherapeutic and chemopreventive agents. Med Princ Pract 25(Suppl. 2): 41–59. DOI: 10.1159/000443404.

Cunningham JJ, Gatenby RA, Brown JS (2011). Evolutionary dynamics in cancer therapy. Mol Pharm 8(6): 2094–2100. DOI: 10.1021/mp2002279.

Dasari R, Banuls LMY, Masi M, Pelly SC, Mathieu V, Green IR, et al. (2014). C1,C2-ether derivatives of the Amaryllidaceae alkaloid lycorine: Retention of activity of highly lipophilic analogues against cancer cells. Bioorganic Med Chem Lett 24(3): 923–927. DOI: 10.1016/j.bmcl.2013.12.073.

Duque L, Bravo K, Osorio E (2017). A holistic anti-aging approach applied in selected cultivated medicinal plants: A view of photoprotection of the skin by different mechanisms. Ind Crops Prod 97: 431–439. DOI: 10.1016/j.indcrop.2016.12.059.

Gordon R (2013). Skin cancer: An overview of epidemiology and risk factors. Semin Oncol Nurs 29(3): 160–169. DOI: 10.1016/j.soncn.2013.06.002.

Gonring-Salarini K, Conti R, de Andrade JP, Borges BJ, Aguiar AC, de Souza J, et al. (2019). *In vitro* antiplasmodial activities of alkaloids isolated from roots of *Worsleya procera* (Lem.) Traub (Amaryllidaceae). J Braz Chem Soc 30(8): 51–58. DOI: 10.21577/0103-5053.20190061.

Howes MJR (2018). The evolution of anticancer drug discovery from plants. Lancet Oncol 19(3): 293–294. DOI: 10.1016/S1470-2045(18)30136-0.

Ingrassia L, Lefranc F, Dewelle J, Pottier L, Mathieu V, Spiegl-Kreinecker S, et al. (2009). Structure-activity relationship analysis of novel derivatives of narciclasine (an Amaryllidaceae isocarbostyril derivative) as potential anticancer agents. J Med Chem 52(4): 1100–1114. DOI: 10.1021/jm8013585.

Kornienko A, Evidente A (2008). Chemistry, biology, and medicinal potential of narciclasine and its congeners. Chem Rev 108(6): 1982–2014. DOI: 10.1021/cr078198u.

Kozma B, Eide MJ (2014). Photocarcinogenesis: An epidemiologic perspective on ultraviolet light and skin cancer. Dermatol Clin 32(3): 301–313. DOI: 10.1016/j.det.2014.03.004.

Kucheryavskiy S (2021). Getting started with mdatools for R. [online] [cit. 2021-11-20]. Available from: https://mdatools.com/docs/

Lee JH, An HT, Chung JH, Kim KH, Eun HC, Cho KC (2002). Acute effects of UVB radiation on the proliferation and differentiation of keratinocytes. Photodermatol Photoimmunol Photomed 18(5): 253–261. DOI: 10.1034/j.1600-0781.2002.02755.x.

Lee WR, Lin YK, Alalaiwe A, Wang PW, Liu PY, Fang JY (2020). Fractional laser-mediated siRNA delivery for mitigating psoriasis-like lesions via IL-6 silencing. Mol Ther Nucleic Acids 19: 240–251. DOI: 10.1016/j.omtn.2019.11.013.

Lianza M, Verdan MH, de Andrade JP, Poli F, de Almeida LC, Costa-Lotufo LV, et al. (2020). Isolation, absolute configuration and cytotoxic activities of alkaloids from *Hippeastrum goianum* (Ravenna) Meerow (Amaryllidaceae). J Braz Chem Soc 31: 2135–2145. DOI: 10.21577/0103-5053.20200116.

Lu JJ, Wang YT (2020). Identification of anti-cancer compounds from natural products. Chin J Nat Med 18(7): 481–482. DOI: 10.1016/S1875-5364(20)30057-1.

Maier MJ (2015). Package 'REdaS'. [online] [cit. 2021-11-20]. Available from: https://cran.r-project.org/web/packages/REdaS/REdaS.pdf

Masi M, Van Slambrouck S, Gunawardana S, van Rensburg MJ, James PC, Mochel JG, et al. (2019). Alkaloids isolated from *Haemanthus humilis* Jacq., an indigenous South African Amaryllidaceae: Anticancer activity of coccinine and montanine. South African J Bot 126: 277–281. DOI: 10.1016/j.sajb.2019.01.036.

Mevik BH, Wehrens R, Liland KH, Hiemstra P (2019). Package 'pls': Partial least squares and principal component regression. [online] [cit. 2021-11-20]. Available from: https://github.com/bhmevik/pls

Montes de Oca MK, Pearlman RL, McClees SF, Strickland R, Afaq F (2017). Phytochemicals for the prevention of photocarcinogenesis. Photochem Photobiol 93(4): 956–974. DOI: 10.1111/php.12711.

Muramatsu S, Kubo R, Nishida E, Shintani Y, Morita A (2016). Serum interleukin-6 levels in response to biologic treatment in patients with psoriasis. Mod Rheumatol 27(1): 137–141. DOI: 10.3109/14397595.2016.1174328.

Nair JJ, Bastida J, van Staden J (2016b). *In vivo* cytotoxicity studies of Amaryllidaceae alkaloids. Nat Prod Commun 11(1): 121–132.

Nair JJ, Bastida J, Viladomat F, van Staden J (2012). Cytotoxic agents of the crinane series of Amaryllidaceae alkaloids. Nat Prod Commun 7(12): 1677–1688.

Nair JJ, van Staden J, Bastida J (2016a). Cytotoxic alkaloid constituents of the Amaryllidaceae. Stud Nat Prod Chem 49: 107–156. DOI: 10.1016/B978-0-444-63601-0.00003-X.

Newman DJ, Cragg GM (2020). Natural products as sources of new drugs over the nearly four decades from 01/1981 to 09/2019. J Nat Prod 83(3): 770–803. DOI: 10.1021/acs.jnatprod.9b01285.

Nichols JA, Katiyar SK (2010). Skin photoprotection by natural polyphenols: Anti-inflammatory, antioxidant and DNA repair mechanisms. Arch Dermatol Res 302(2): 71–83. DOI: 10.1007/s00403-009-1001-3.

Nieweg OE, Gallegos-Hernández JF (2016). Cutaneous melanoma and the new drugs. Cir Cir (English Ed) 83(2): 175–180. DOI: 10.1016/j.circen.2015.08.016.

Oak ASW, Athar M, Yusuf N, Elmets CA (2018). UV and Skin: Photocarcinogenesis. In: Environment and Skin. Switzerland: Springer International Publishing. pp. 67–103. DOI: 10.1007/978-3-319-43102-4_8.

Qiao P, Guo W, Ke Y, Fang H, Zhuang Y, Jiang M, et al. (2019). Mechanical stretch exacerbates psoriasis by stimulating keratinocyte proliferation and cytokine production. J Invest Dermatol 139(7): 1470–1479. DOI: 10.1016/j.jid.2018.12.019.

Qiu S, Sun H, Zhang AH, Xu HY, Yan GL, Han Y, Wang XJ (2014). Natural alkaloids: Basic aspects, biological roles, and future perspectives. Chin J Nat Med 12(6): 401–406. DOI: 10.1016/S1875-5364(14)60063-7.

Real FX, López C (2016). Medicina Interna. Madrid: Elsevier, pp. 1191–1202.

Reuter S, Gupta SC, Chaturvedi MM, Aggarwal BB (2010). Oxidative stress, inflammation, and cancer: How are they linked? Exp Ther 49(11): 1603–1616. DOI: 10.1016/j.freeradbiomed.2010.09.006.

Roussi F, Gueritte F, Fahy J (2012). The vinca alkaloids. In: Cragg GM, Kingston DGI, Newman DJ (Eds). Anticancer agents from natural products. Second ed. CRC/Taylor & Francis, Boca Raton, pp. 177–198.

Sung H, Ferlay J, Siegel RL, Laversanne M, Soerjomataram I, Jemal A, Bray F (2021). Global cancer statistics 2020: GLOBOCAN estimates of incidence and mortality worldwide for 36 cancer in 185 countries. CA Cancer J Clin 71(3): 209–249. DOI: 10.3322/caac.21660.

Traykova M, Traykov T, Hadjimitova V, Krikorian K, Bojadgieva N (2003). Antioxidant properties of galantamine hydrobromide. Z Naturforsch C J Biosci 58(5–6): 361–365. DOI: 10.1515/znc-2003-5-613.

Voiculescu VM, Lisievici CV, Lupu M, Vajaitu C, Draghici CC, Popa AV, et al. (2019). Mediators of inflammation in topical therapy of skin cancers. Mediators Inflamm 2019: 8369690. DOI: 10.1155/2019/8369690.

Wang C, Wang Q, Li X, Jin Z, Xu P, Xu N, et al. (2016). Lycorine induces apoptosis of bladder cancer T24 cells by inhibiting phospho-Akt and activating the intrinsic apoptotic cascade. Biochem Biophys Res Commun 483(1): 197–202. DOI: 10.1016/j.bbrc.2016.12.168.

Wu D, Yotnda P (2011). Production and detection of reactive oxygen species (ROS) in cancers. J Vis Exp (57): e3357. DOI: 10.3791/3357.

Ying X, Huang A, Xing Y, Lan L, Yi Z, He P (2017). Lycorine inhibits breast cancer growth and metastasis via inducing apoptosis and blocking Src/FAK-involved pathway. Sci China Life Sci 60(4): 417–428. DOI: 10.1007/s11427-016-0368-y.